Results of the Deep Space Atomic Clock Deep Space Navigation Analog Experiment

Conference Paper · August 2020

CITATIONS
6

READS
427

3 authors, including:

Jill Seubert
California Institute of Technology
19 PUBLICATIONS **185** CITATIONS
SEE PROFILE

Todd Ely
California Institute of Technology
95 PUBLICATIONS **1,351** CITATIONS
SEE PROFILE

AAS 20-440

RESULTS OF THE DEEP SPACE ATOMIC CLOCK DEEP SPACE NAVIGATION ANALOG EXPERIMENT

Jill Seubert[*], Todd Ely[†], Jeffrey Stuart[‡]

The timing and frequency stability provided by the Deep Space Atomic Clock (DSAC) is almost comparable with the Deep Space Network's ground clocks, and will enable one-way radiometric measurements with accuracy equivalent to current two-way tracking data. A demonstration unit of the clock was launched into low Earth orbit on June 25, 2019, for the purpose of validating DSAC's performance in the space environment. GPS data collected throughout the mission was utilized not only for precise clock estimation, but also as a proxy for deep space tracking data to conduct the Deep Space Navigation Analog Experiment. Through careful processing of GPS Doppler data and limited modeling fidelity representative of deep space navigation capabilities, the analog orbit solutions are compared to higher-fidelity solutions, demonstrating DSAC's viability as a navigation instrument in conditions typical for a low altitude Mars orbiter.

INTRODUCTION

The practicality of deep space navigation based solely on one-way radiometric tracking data is currently limited by the performance of the onboard clock. Compared to the very high stability and accuracy of ground atomic clocks (the National Institute of Standards and Technology's Ytterbium lattice atomic clock exhibits white frequency errors with a one-day Allan Deviation (AD) $<$ 1e-17), the performance of space-flown clocks has been lacking.[1] Ultra Stable Oscillators (USOs) exhibit long-term frequency drift that is highly correlated with the orbital parameters, and recovering large clock bias and drift terms following long periods without tracking yields significant degradations in orbit solution quality. The Deep Space Atomic Clock (DSAC) project is a NASA Technology Demonstration Mission (TDM) that has bridged the gap between ground and space clocks by demonstrating the on-orbit performance of a small, low-mass mercury ion ($^{199}Hg^{+}$) atomic clock. In contrast to a USO's frequency drift, DSAC's frequency stability improves over long integration times, providing long-term stability and accuracy almost comparable with the ground clocks in use at the Deep Space Network (DSN). Such a small spacecraft clock error enables one-way X-band and Ka-band radiometric tracking data with accuracy equivalent to current two-way tracking data, allowing a shift to a more efficient and flexible one-way deep space navigation architecture.

The DSAC mission is a hosted payload onboard the General Atomics Orbital Test Bed (OTB) spacecraft, which launched into low Earth orbit (LEO) on June 25, 2019. DSAC's space-based

[*]Deputy Principal Investigator, Deep Space Atomic Clock Technology Demonstration Mission, Jet Propulsion Laboratory, California Institute of Technology, 4800 Oak Grove Drive, Pasadena, CA 91109.

[†]Principal Investigator, Deep Space Atomic Clock Technology Demonstration Mission, Jet Propulsion Laboratory, California Institute of Technology, 4800 Oak Grove Drive, Pasadena, CA 91109.

[‡]Investigation System Engineer, Deep Space Atomic Clock Technology Demonstration Mission, Jet Propulsion Laboratory, California Institute of Technology, 4800 Oak Grove Drive, Pasadena, CA 91109.

performance was characterized via a six-month demonstration, during which Global Positioning System (GPS) tracking data was processed to produce precise orbit and clock solutions. DSAC performed at its anticipated level, and its utility for one-way radiometric deep-space navigation has been validated by showing that orbit determination performance using the one-way data is nearly as accurate as its traditional two-way counterpart. The Deep Space Navigation Analog Experiment utilized the flight GPS tracking data to demonstrate orbit determination performance using one-way and pseudo two-way GPS Doppler data with measurement quality, quantity, and schedule characteristics (such as tracking data density, duration and geometric variability) that are operationally similar to that which is typically available in deep space navigation. This paper presents the detailed methodology of this navigation analog experiment, along with orbit estimation performance using one-way and pseudo two-way GPS Doppler measurements.

DSAC TECHNOLOGY DEMONSTRATION MISSION

The DSAC TDM verified the clock's space performance and demonstrated the viability of $^{199}Hg^{+}$ atomic space clock technology for navigation purposes. DSAC technology uses the stability of the mercury ions' hyperfine transition frequency at 40.5 GHz to effectively steer the frequency output of a quartz crystal USO to a near-constant value.[2] The mercury ions are confined in a trap with applied electric fields and protected from perturbations via applied magnetic fields and shielding. This provides a stable environment for measuring the hyperfine transition very accurately and minimizes sensitivity to temperature and magnetic variations that will be encountered on orbit. Given this enhanced clock stability and the fact that the system has almost no expendables, the DSAC clock technology is suitable for very long-duration space missions. Following a successful yearlong TDM, the clock technology will be advanced from a Technology Readiness Level (TRL) 5 to TRL 7.

The General Atomics OTB spacecraft was launched into a near-circular, near-equatorial orbit by a SpaceX Falcon Heavy rocket, as a secondary payload of the United States Air Force Space Technology Program II. The nominal deployed OTB spacecraft configuration and orbital orientation are shown in Figure 1. The spacecraft mass is $\approx$ 180 kg, it has no active propulsion system and is nominally oriented with the solar arrays pointed in the zenith direction. The demonstration DSAC's size, weight, and average power are 29 cm x 26 cm x 23 cm, 16.5 kg, and 46.6 W, respectively. Figure 2 shows a computer model of DSAC on the left and the assembled flight hardware on the right (mounted to baseplate). In addition to the atomic clock demonstration unit, the DSAC payload also includes an oversized crystal USO and a GPS system comprised of a JPL-designed TriG Precise Orbit Determination (POD) receiver and a zenith-pointing choke ring antenna (antenna shown in Figure 1).

Throughout the first six months of the demonstration mission, the GPS subsystem collected L1 and L2 GPS phase and pseudo-range measurements for use in satisfying the two primary objectives of the DSAC TDM: to verify the clock's stability and drift with an AD $<$ 2.0e-14 at one day while in orbit, and to demonstrate the clock's viability as a navigation tool by reconstructing the orbit to within 10 m uncertainty (3σ) in a tracking and data configuration analogous to deep space operations. The flight performance of the clock over the timespan of this analysis was $\approx$ 1e-14 at one day, with later clock performance improved by nearly an order of magnitude. The clock telemetry is currently being monitored to verify longer duration health and status, with intermittent GPS data processing to assess longer-term clock performance (beyond the mission requirement).

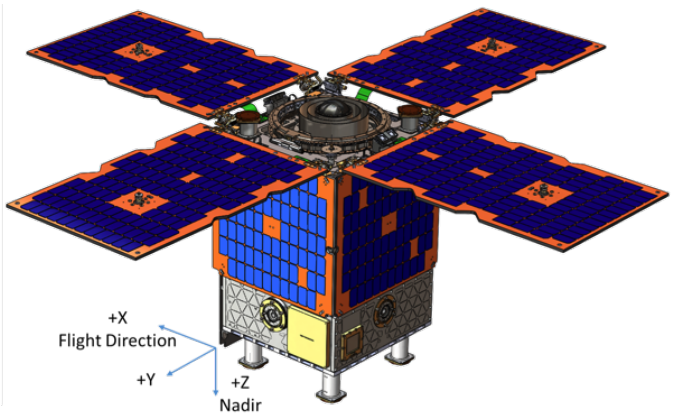

Figure 1. Nominal deployed OTB spacecraft configuration and on-orbit orientation (figure provided by SST-US).

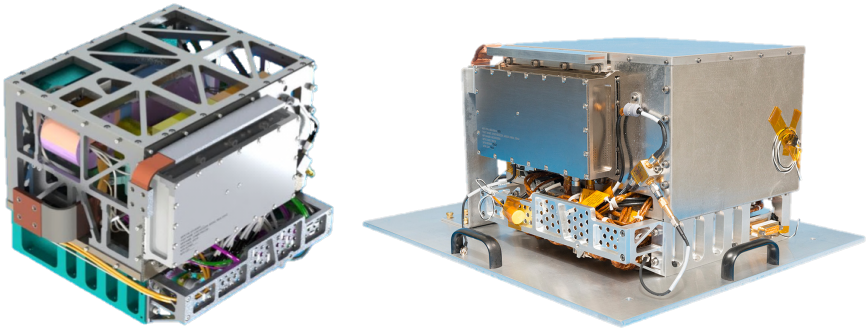

Figure 2. DSAC payload CAD model (left) and assembled flight hardware (right).

OTB Orbital Environment and Models

DSAC's performance will be evaluated in the LEO space environment, and as such evaluation of the clock performance will necessitate high-fidelity models of the orbital dynamics and GPS measurements. Additionally, the expected modeling errors that will be encountered on orbit must be characterized. Reference 3 presents detailed information regarding the nominal dynamic and measurement environment and expected errors. A brief summary is provided here.

The set of high-fidelity dynamic models applied during numerical integration of the OTB trajectory include the 360 x 360 GRACE gravity model GGM05C,[4] Earth gravitational tide models (solid tide, ocean convolution tide, spectral air tide, mean pole tide), Newtonian luni-solar gravity, solar radiation pressure, atmospheric drag with the Drag Temperature Model (DTM)-2012 density model, and Earth albedo and thermal emissivity pressure. The solar radiation pressure and atmospheric drag accelerations depend on a model of the OTB spacecraft; this model is comprised of 8 flat plates, representing the six-sided bus and solar array topsides and undersides, and oriented in the nominal spacecraft-fixed frame as shown in Figure 1. The diffuse and specular reflectivity properties of all

major surface materials have been provided by SST-US and are included in the nominal spacecraft model. The spacecraft attitude is modeled via quaternions estimated by the onboard attitude Kalman filter and reported in daily telemetry.

The GPS pseudo-range and phase measurement models include the geometric range from the GPS transmit antenna to the OTB choke ring antenna, transmitter and receiver clocks, antenna locations and phase center offsets, multipath (carrier phase and pseudo-range models were empirically constructed during the on-orbit commissioning phase), GPS receiver temperature effects, and phase wind up. The GPS satellite orbits and clocks are defined by the Jet Propulsion Laboratory Analysis Center's publicly-available Rapid data products. Single-frequency (L1 and L2) data are linearly combined to produce first-order ionosphere-free carrier-phase and pseudo-range measurements.

The local spacecraft time, including time dilation due to relativistic effects, is numerically integrated along with the trajectory. The spacecraft time frame (T_{SC}) offset from Ephemeris Time (T_{ET}) is modeled as a function of the spacecraft gravitational potential (U) and geocentric inertial spacecraft velocity (v) via:[5]

$$\frac{\partial T_{SC} - T_{ET}}{\partial t} = L - \frac{1}{c^2}\left(U + \frac{v^2}{2}\right) \tag{1}$$

The initial rate ($L = 0.06969290134x10^{-8}$) used for this analysis is published in Reference 6. Accordingly, the gravitational potential U as implemented in Eq. 1 includes Earth's GM and J2 effects only; high-order spherical harmonics, tidal effects, and luni-solar gravity are removed for time frame integration.

The OTB spacecraft passes through the South Atlantic Anomaly approximately 6 to 8 times per day. Though the passage through this intense radiation flux environment can be observed directly via internal clock telemetry, there is no net effect on the clock performance or the Deep Space Navigation Analog Experiment results.

DEEP SPACE NAVIGATION ANALOG EXPERIMENT

The primary objectives of the DSAC mission include not only demonstrating the clock performance in the space environment, but also demonstrating that the DSAC instrument can be used for radiometric deep space navigation purposes. In lieu of directly demonstrating this capability in deep space, the Deep Space Navigation Analog Experiment processes the Earth-orbit flight data in a manner that mimics orbit reconstruction of a low-altitude Mars orbiter. Careful selection of GPS data, combined with artificial data degradation and appropriate data weighting, allows for a demonstration of orbit determination that is analogous to that of the Mars Reconnaissance Orbiter (MRO). The navigation analog experiment is performed using the same software package currently used for operational deep space navigation.

Methodology

The base navigation analog experiment to demonstrate DSAC's utility as a deep space navigation tool was performed as summarized below. The flight data selected for the results presented here spans 30-SEP-2019 00:00:00 GPS through 02-OCT-2019 00:00:00 GPS. A 48 hour data span is typical for MRO orbit reconstruction. For MRO operations, orbit overlaps on the order of 12 hours are used for assessment of solution consistency; for the navigation analog experiment, the orbit

solution may be compared directly to that estimated using the full set of GPS carrier phase and pseudo-range tracking data and the highest-fidelity models available. (This orbit solution is referred to as the "truth" solution.)

Details regarding the data degradation and downselection, conversion of carrier phase to Doppler data, injection of frame model errors and the navigation filter configuration are presented in the following subsections.

1. Estimate "Truth" OTB orbit and DSAC clock using full set of GPS carrier phase and pseudo-range data
2. Degrade GPS carrier-phase and pseudo-range data with simulated media errors
3. Downselect degraded GPS carrier-phase data to represent DSN tracking of a Mars orbiter
4. Convert downselected GPS carrier-phase data to GPS Doppler data
5. Degrade Earth fixed frame model with simulated Earth Orientation Parameter errors
6. Process GPS Doppler data with navigation filter
7. Compare converged orbit solution to "truth" orbit

Data Degradation

The DSAC GPS receiver collects dual frequency (L1 and L2) carrier phase and pseudo-range tracking data, which is linearly combined to remove first-order ionospheric errors from the tracking data. Furthermore, at an altitude of 720 kilometers the spacecraft is well above the troposphere. Tracking data with no media effects (to first order) is desired for optimal clock and orbit estimation, but is not realistically representative of the quality of radiometric tracking data collected to support deep space navigation. In reality, radiometric tracking signals passing between the Deep Space Network (DSN) ground stations and the spacecraft they support must traverse both the troposphere, ionosphere, and solar plasma. Dual-frequency tracking to remove first-order ionospheric and solar plasma errors is not standard practice. Though tropospheric and ionospheric calibrations are routinely used for ground-based navigation, the calibrations include residual errors that cannot be removed from the raw tracking data. The exponentially correlated random variable (ECRV) stochastic models shown in Table 1 represent the residual media errors, with the ionosphere uncertainties reported at the X-band frequency of 8.4 GHz, with all uncertainties representing a two-way signal transit. The troposphere error levels assume zenith ground antenna pointing, while ionosphere errors are modeled along the line-of-sight. Troposphere errors are characterized by dry and wet components, while ionosphere errors are characterized by local day and night.[7] (Note, solar plasma effects on the signal are typically handled via adjusted data weights or data pre-whitening.)[8]

Simulated media errors representing the residual error remaining after applying empirical media calibrations were realized by generating four independent ECRV random processes for the troposphere and ionosphere components. To simulate the random processes for one-way signal transits, the uncertainty values shown in Table 1 were scaled by $\frac{1}{\sqrt{2}}$, assuming uncorrelated uplinks and downlinks for deep space light times.

The raw dual-frequency carrier phase and pseudo-range measurements are degraded with the simulated media errors. The total zenith troposphere error is comprised of both the dry and wet

Table 1. Residual Tropospheric and Ionospheric Error Stochastic Models

Parameter	Stochastic Model	Uncertainty (1-σ)
Troposphere, Dry	ECRV, τ = 6 hours	0.16 cm
Troposphere, Wet	ECRV, τ = 6 hours	1 cm
Ionosphere, Day	ECRV, τ = 6 hours	26 cm
Ionosphere, Night	ECRV, τ = 6 hours	26 cm

troposphere components and mapped to the tracking signal line of sight via a $\frac{1}{\sin(el)}$ scaling, where *el* denotes the transmitting GPS satellite's elevation as seen from OTB's local horizontal/local vertical plane. The line-of-sight ionosphere error is a function of the mean local solar time at the OTB spacecraft. The ionosphere error is added to the pseudo-range measurement but subtracted from the carrier phase measurement to represent code delay and phase advance; the troposphere error is added to both. In order to isolate the effects of onboard clock errors, all one-way and pseudo two-way GPS Doppler measurements were degraded with identical media error realizations. While this does under-represent the media errors present in a two-way radio signal, appropriate data weighting accounts for the increased two-way measurement uncertainty.

Data Downselection

Tracking data of an Earth orbiting satellite from the full GPS constellation provides a rich geometric diversity in a short period of time; GPS signals as observed by the spacecraft receiver rise and set in a matter of minutes, originate from six unique orbital planes, and (for the OTB spacecraft) track on average nine satellites at one time. In contrast, DSN tracking of a spacecraft in deep space suffers severely limited geometric variation. For example, DSN tracking signals as observed by a Mars orbiter such as MRO appear to originate from a relatively fixed inertial point over a span of a few days; the signals originate from approximately a single orbital plane and primarily from a single ground station at a time. Furthermore, GPS tracking of an Earth orbiter is continuous, whereas DSN tracking of a Mars orbiter includes lengthy (8-10 hour) tracking gaps when the DSN is committed to tracking other spacecraft.

To better represent the limited duration, density and geometric variability of DSN tracking, GPS tracking data is carefully downselected to a more limited data set. As shown in Figure 3, GPS tracking data is constrained to originate from a single GPS orbital plane designation, and within a small angular constraint of the GPS orbit ascending node crossing. The angular constraint is defined as the amount of DSN ground station angular rotation seen by a low-altitude Mars orbiter over one orbit, denoted by ω in Figure 4. Assuming a Martian circular orbit with a period of 100 minutes, which must be noted is commensurate with OTB's orbit but is not physically possible for a Martian satellite, the worst-case DSN visibility will result is approximately 50 minutes of tracking per orbit. This bounding case results in a DSN subtended angle of 12.5 degrees; as such, the GPS tracking data is constrained to originate from within +/- 6.25 degrees of the ascending node crossing. Note that the angular constraint shown in Figure 3 was arbitrarily chosen for illustrative purposes and is not reflective of the applied constraint.

The analysis presented herein downselected the GPS carrier phase and pseudo-range tracking data to the GPS orbital plane designated "B". Over the 48 hour data set processed for this analysis, the "B" plane was populated by 5 active GPS satellites. Figure 5 shows the carrier phase postfit

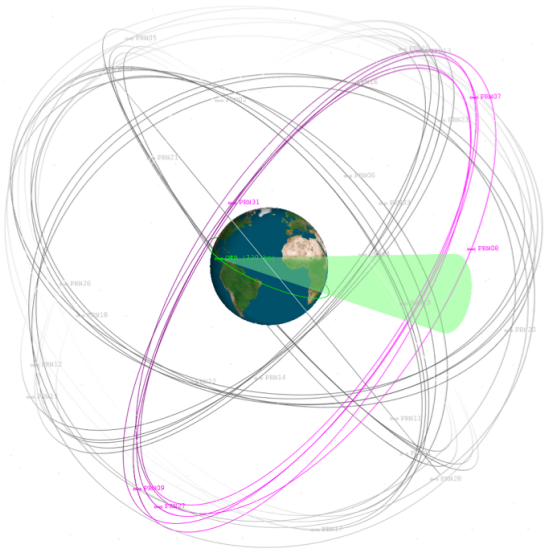

Figure 3. Illustration of GPS tracking data selection to better represent DSN tracking of a low-altitude Mars orbiter. Observability cone half-angle arbitrarily chosen for illustrative purposes.

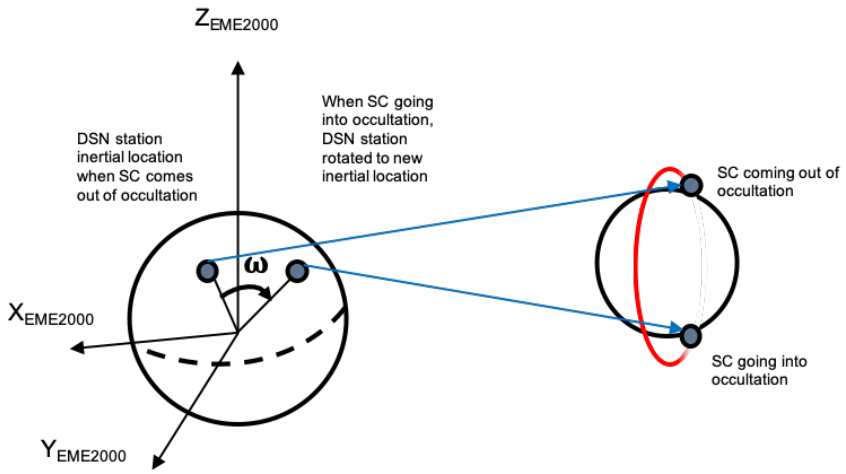

Figure 4. Per-Orbit DSN angular rotation as seen by a low-altitude Mars orbiter.

residuals from the "truth" clock and orbit estimation, which illustrates the density of the full set of GPS carrier phase data. The reduced data set after downselection to the "B" plane and constraining the data to within +/- 6.25 degrees of the ascending node crossing is illustrated by the Doppler postfit residuals shown in Figure 6. The reduction of GPS tracking data from the full set of carrier phase and pseudo-range tracking data to the downselected Doppler tracking data leaves approximately 0.2% of the original data for utility in the Navigation Analog experiment.

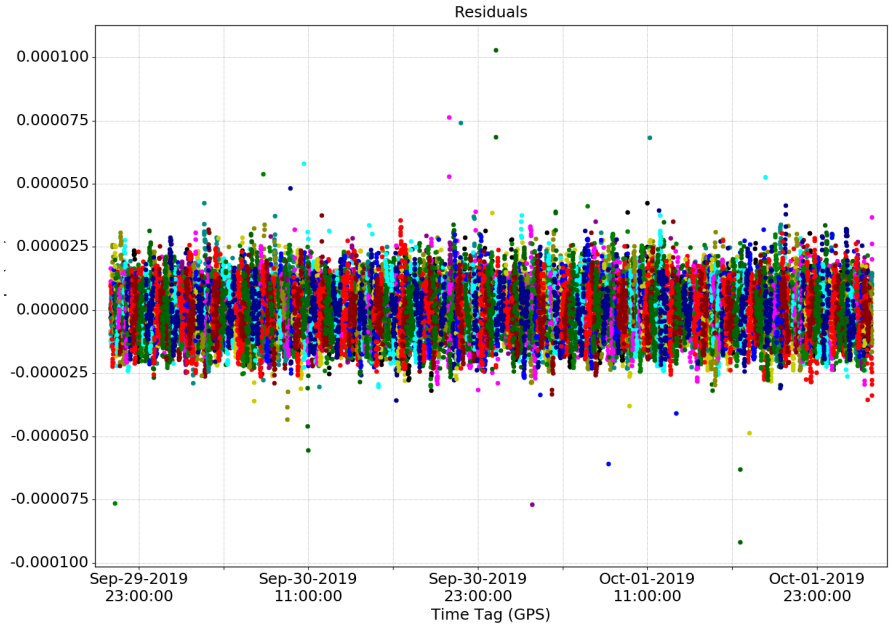

Figure 5. GPS carrier phase postfit residuals (full GPS tracking, colors denote GPS transmitters).

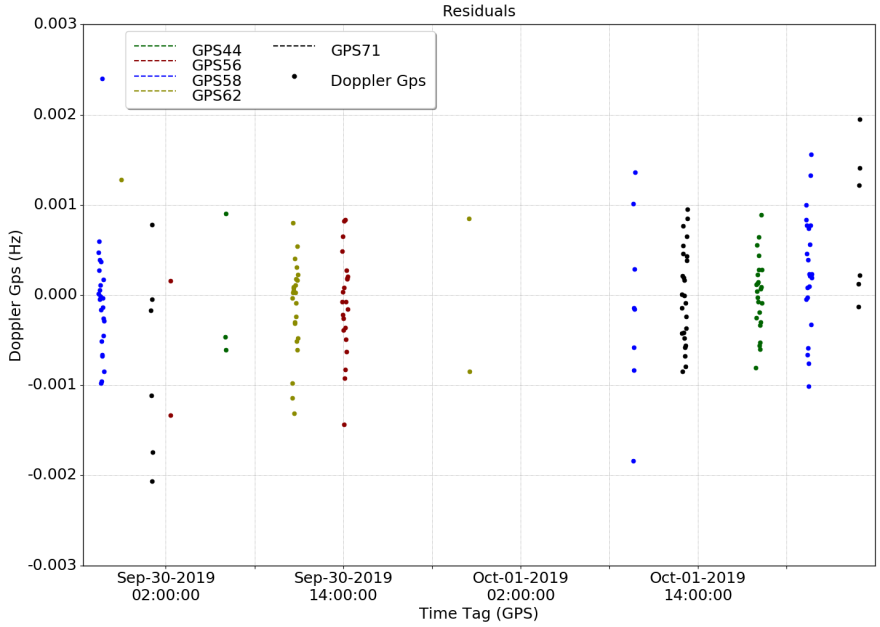

Figure 6. Downselected GPS Doppler postfit residuals (pseudo two-way Doppler).

GPS Doppler Measurements

The downselected GPS carrier phase measurements are converted into Doppler space to reflect current DSN radiometric tracking. This conversion is performed by differencing the degraded (e.g. media corrupted) phase measurements ($\phi(t)$) and averaging over the integration time (T). The average differenced phase is then converted from velocity space to frequency space via scaling by the ratio of the GPS signal frequency (f_{LC}, the linear combination of L1 and L2 frequencies) to the speed of light (c). The full conversion is shown in Equation 2. This analysis utilized a Doppler integration time of 60 seconds, which is typical for Mars orbiter trajectory reconstruction.

$$\Delta f(t-\frac{T}{2}) = \frac{f_{LC}}{cT}\Big(\phi(t)-\phi(t-T)\Big) \tag{2}$$

The GPS phase measurements include both transmitter and receiver clock error, as shown in Equation 3, in which ρ is the signal transit light time, δt_r is the receiver clock error and δt_t is the transmitter (GPS) clock error. By applying the JPL Analysis Center GPS clock solutions, the transmitter clock errors are reduced to a level below the phase measurement noise. In contrast, the receiver clock errors are entirely manifested in the one-way GPS Doppler (Equation 4). The one-way GPS Doppler is therefore directly analogous to uplink one-way DSN Doppler, in which the DSN transmitter clock error is negligible but the onboard clock error still contributes to the measurement.

$$\phi(t) = c\Big(\rho(t)+\delta t_r(t)-\delta t_t(t-\rho(t))\Big) \tag{3}$$

$$\phi_{F1}(t) = c\Big(\rho(t)+\delta t_r(t)-\delta t_t(t-\rho(t))+\delta t_t^*(t-\rho(t))\Big) \approx c\Big(\rho(t)+\delta t_r(t)\Big) \tag{4}$$

As GPS is a transmit-only navigation system, it is not possible to collect true two-way measurements during DSAC's on-orbit operations. Two-way Doppler data differs from one-way Doppler data in several significant ways. For two-way DSN data, transmitted and received at DSN ground antennas, the onboard clock error does not contribute to the measurement. As the two-way measurements are derived from the round-trip light time as compared to the one-way light time, the measurement sensitivity to the estimated dynamic state is scaled by a factor of 2. Finally, for frequencies such as S- and X-band where the radiometric signal noise is dominated by uncorrelated path-dependent effects, two-way measurements are a factor of $\sqrt{2}$ noisier than one-way measurements. Considering these points, one-way GPS Doppler can be manipulated such that it may serve as a surrogate for true two-way Doppler data. The combined effect of increased measurement noise and increased measurement sensitivity may be handled by scaling the nominal one-way data weight by a factor of $\sqrt{2}$. The onboard clock error may be removed or reduced via calibration, which leads to the concept of pseudo two-way GPS Doppler.

In simulation analyses, the truth onboard clock error is known and can therefore be entirely removed from the one-way GPS Doppler measurements; this measurement is now directly analogous to two-way DSN Doppler data, in which the clock errors are not the dominant measurement error source. In actual flight, however, the true onboard clock error is unknown, and thus cannot be completely calibrated out of the one-way GPS Doppler data. As a proxy, the estimated onboard ("truth") clock solution can be removed from the one-way GPS phase data, creating pseudo two-way GPS

phase measurements (ϕ_{pF2}) in which only the residual clock error remains (Equation 5). Though in actuality both data types are physically one-way measurements, comparisons of navigation performance utilizing one-way GPS Doppler and pseudo two-way GPS Doppler provide insight into the navigation performance were true two-way tracking data possible.

$$\phi_{pF2}(t) = c\Big(\rho(t) + \delta t_r(t) - \delta t_t(t-\rho(t)) - \delta t_r^*(t) + \delta t_t^*(t-\rho(t))\Big) \approx c\Big(\rho(t)\Big) \tag{5}$$

The one-way GPS Doppler data weight determined by converting 1 centimeter of phase noise to the Doppler domain, resulting in a data noise of approximately 2.204 mHz (0.23 mm/sec). Scaling by $\frac{1}{\sqrt{2}}$, the pseudo two-way GPS Doppler data weight is approximately 1.558 mHz (0.08 mm/sec).

Earth Orientation Model Degradation

Deep space navigation must also contend with errors in the modeled orientation of the Earth-fixed reference frame relative to the inertial reference frame, either estimating or considering errors in the Earth's pole orientation and UT1 time frame.[5] Errors in the fixed-frame pointing of the Earth's pole, assuming the Z direction is aligned with the pole, and UT1 time frame were simulated much like the residual media errors; Table 2 presents the stochastic models utilized to generate random realizations of the Earth orientation parameter errors. The error levels shown in the table represent residual errors after high-fidelity calibrations have been applied.[7]

Table 2. Residual Earth Orientation Parameter Error Stochastic Models

Parameter	Stochastic Model	Uncertainty (1-σ)
Pole Orientation (X)	ECRV, τ = 48 hours	2 cm
Pole Orientation (Y)	ECRV, τ = 48 hours	2 cm
UT1 Time Frame	ECRV, τ = 48 hours	5 cm

Unlike the simulated media errors, the simulated Earth orientation parameter errors are not applied to the raw measurements as the true Earth orientation at the time of the data collection is unknown. The simulated errors were instead applied to the navigation analog filter's nominal Earth fixed frame, thus degrading the nominal model.

Navigation Filter Configuration

The navigation analog upper-diagonal sequential Kalman filter configuration is shown in Table 3. In addition to the initial spacecraft position and velocity states, the filter states include corrections to several dynamic modeling errors. A bias correction to the drag coefficient and a constant scale factor on the solar pressure are estimated to account for mis-modeling of the spacecraft bus and solar flux activity. Additional states compensate for observed empirical acceleration mismodeling, which is dominant in the orbital normal direction. It is theorized that this observed spacecraft acceleration is due to reradiation thermal effects, as the acceleration is aligned with the spacecraft radiator. The filter has been empirically tuned to estimate an orbital acceleration (Equation 6, in which P denotes orbital period and t_0 is the initial epoch) in the normal direction, as well as stochastic accelerations in the spacecraft-fixed reference frame. The filter includes only one accommodation for the one-way data processing, which is to add a clock drift estimate every nine hours (approximating DSN

station acquisition for a Mars orbiter). This is necessary because of small frequency offsets that would exist between transmitting and receiving hardware.

$$a_N(t) = A\sin\left(2\pi\frac{t-t_0}{P}\right) + B\cos\left(2\pi\frac{t-t_0}{P}\right) \tag{6}$$

Table 3. Navigation Analog Experiment Filter Configuration

Estimated Parameter	Parameter Type	*a priori* Uncertainty (1-σ)
Position (EME2000)	Dynamic	10 m
Velocity (EME2000)	Dynamic	1 cm/sec
OTB Drag Coefficient	Bias	0.25 (10%)
OTB Solar Pressure Scale Factor	Bias	0.1 (10%)
Orbital Acceleration Coefficients	Bias	10 pm/sec^2
Empirical Acceleration (Radial)	Stochastic (ECRV, τ = 600 sec Batch duration = 60 sec)	2 pm/sec^2
Empirical Acceleration (Tangential)	Stochastic (ECRV, τ = 600 sec Batch duration = 60 sec)	10 pm/sec^2
Empirical Acceleration (Normal)	Stochastic (ECRV, τ = 600 sec Batch duration = 60 sec)	15 pm/sec^2
Clock drift (one-way GPS Doppler only)	Stochastic (White, Batch duration = 9 hrs	1e-9

RESULTS

The navigation analog experiment was conducted using both pseudo two-way and one-way GPS Doppler measurements, respectively. This allows for a direct investigation into the effect of the onboard clock stochastic behavior on orbit reconstruction. As described in the following section, a calibration of the onboard clock deterministic time offset and rate must be performed for optimal orbit reconstruction. All results presented here represent the smoothed results of a converged upper-diagonal sequential Kalman filter.

As will be shown, both the tangential and normal components of the covariance matrix are significant; hence it is necessary to decompose the covariance matrix into it's principal directional components for a meaningful computation of the three-dimensional uncertainty. Following eigenvalue decomposition, the root sum square (RSS) of the covariance matrix diagonal values is computed; this three-dimensional uncertainty representation is referred to in this paper as σ_{RSS}.

Pseudo Two-Way GPS Doppler

The postfit pseudo two-way GPS Doppler measurement residuals are shown in Figure 6, and demonstrate that the data is able to fit the data very well; the data residuals are Gaussian with an RMS well below the assigned data noise of 1.558 mHz. (This discrepancy indicates that the

data weight, based off a 1 cm GPS carrier phase noise level, is indeed conservative as expected.) Figure 7 presents the differences between the navigation analog orbit solution and the "truth" orbit solution determined using the full GPS constellation. The the 3-σ formal uncertainty bounds shown correspond to the navigation analog solution. These orbit errors are presented in the spacecraft-fixed radial, tangential and orbit normal reference frame. The uncertainty inflation, primarily visible in the tangential direction but observed to a lesser degree in the radial direction as well, is due to the lengthy tracking data gaps over approximately 30-SEP-2019 14:00 GPS through 30-SEP-2019 22:30 GPS (8.4 hours) and 30-SEP-2019 22:30 GPS through 01-OCT-2019 09:30 GPS (11 hours). The three-dimensional 3-σ_{RSS} is 4.452 m in position and 3.969 mm/sec in velocity (not shown). These results are in family with the operational orbit reconstruction performance of MRO.

The pseudo two-way GPS Doppler results demonstrate that the estimated onboard clock solution can be effectively removed from the data, such that orbit reconstruction based on GPS Doppler can be performed at a level commensurate with current low-altitude Mars orbiters. These results establish a baseline against which one-way GPS Doppler performance can be compared.

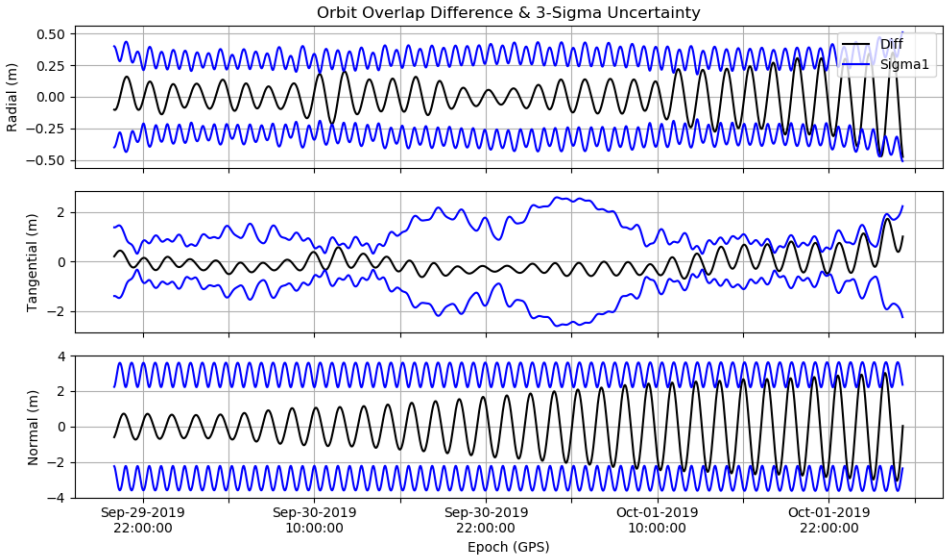

Figure 7. Orbit errors and 3-σ uncertainty envelope (pseudo two-way Doppler).

One-Way GPS Doppler

Recall the three primary differences between pseudo two-way and one-way GPS Doppler include appropriate two-way data weighting, an additional filter state to estimate an onboard clock rate every 9 hours, and the full inclusion of the onboard clock's deterministic and stochastic errors. The postfit residuals and orbit errors using one-way GPS Doppler measurements are shown in Figures 8 and 9, respectively. The postfit residuals are similar to those for the pseudo two-way measurements, showing that the filter is able to fit to the data fairly well. The 3-σ_{RSS} is 8.229 m in position and 6.360 mm/per in velocity; the inflation relative to the pseudo two-way 3-σ_{RSS} is due to the stochastic clock rate filter state, but still in family with current low-altitude Mars orbit reconstruction. However, the orbit solution errors as compared to the "truth" orbit exhibit a bias in the tangential direction of approximately 5 m. The bias is not reflected by the formal solution uncertainty, indicating that the filter - and hence, the orbit analyst - is unaware of this significant bias. Observable in the navigation

analog experiment only because a “truth” orbit may be estimated using the full GPS constellation, the one-way GPS Doppler orbit solution would be problematic for practical navigation purposes.

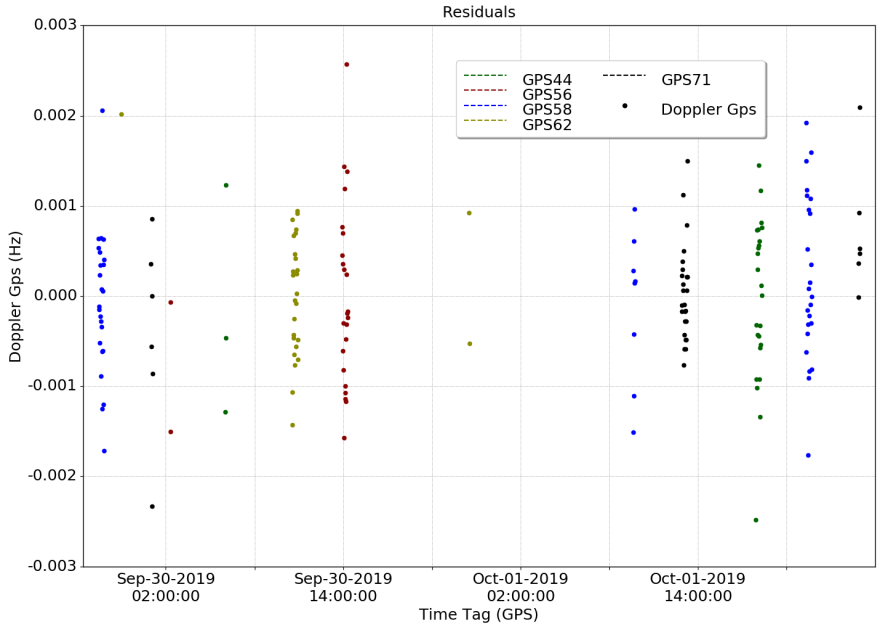

Figure 8. GPS Doppler postfit residuals (one-way Doppler).

Deterministic Clock Calibration

The tangential direction of the OTB-fixed frame is, to first order, equivalent to the along-track direction, and can be due to the aliasing of an onboard clock bias into the orbit solution. Recall that the navigation analog filter as executed here has no means to deal with onboard clock biases. Based on the one-way GPS Doppler results, it is deemed necessary to perform a calibration of the deterministic onboard clock bias and clock rate errors. Clock rate calibration may be conducted using a lengthy set of one-way GPS Doppler data, but Doppler data has very limited observability into the clock bias; a constant clock bias present in the carrier phase measurement is differenced out when constructing differenced phase Doppler measurements, and the residual clock bias effect is through the measurement time tag only. For this reason, it is necessary to include pseudo-range data into the deterministic clock calibration as range measurements possess strong observability of onboard clock bias. The combination of Doppler and range data is routinely collected during navigation operations, though for Mars orbiters the orbit solution depends primarily upon the Doppler data.

The deterministic clock calibration was performed by processing 24 hours of the downselected one-way GPS Doppler data and corresponding pseudo-range data. Both data types were degraded with the simulated media errors, and the filter nominal Earth orientation model was degraded with the simulated stochastic polar motion and UT1 errors. A reduced set of filter states was defined to prioritize estimation of the deterministic clock bias and rate terms over orbit estimation. The reduced filter configuration is shown in Table 4. The deterministic clock bias was estimated to be 0.795215 milliseconds +/- 2 nanoseconds (1-σ), and the deterministic clock rate was estimated to be 1.6 pico-Hz/Hz +/- 1.0 pico-Hz/Hz.

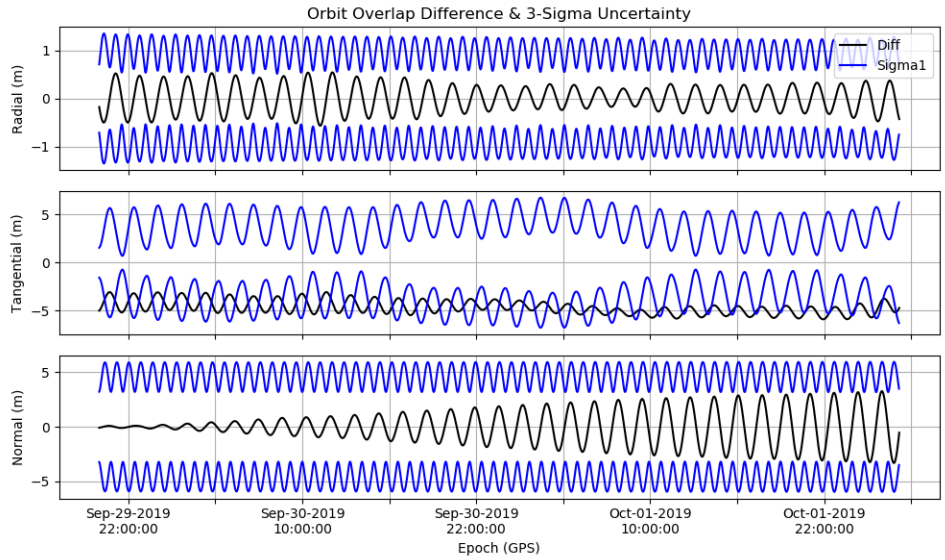

Figure 9. Orbit errors and 3-σ uncertainty envelope (one-way Doppler).

Table 4. Deterministic Clock Calibration Filter Configuration

Estimated Parameter	Parameter Type	*a priori* Uncertainty (1-σ)
Position (EME2000)	Dynamic	10 m
Velocity (EME2000)	Dynamic	1 cm/sec
Clock Offset	Bias	1 msec
Clock Rate	Bias	10 pHz/Hz
Empirical Acceleration (Radial)	Stochastic (ECRV, τ = 600 sec Batch duration = 60 sec)	2 pm/sec^2
Empirical Acceleration (Tangential)	Stochastic (ECRV, τ = 600 sec Batch duration = 60 sec)	10 pm/sec^2
Empirical Acceleration (Normal)	Stochastic (ECRV, τ = 600 sec Batch duration = 60 sec)	15 pm/sec^2

The one-way GPS Doppler analysis was repeated with one small change: the onboard clock model was initialized using the estimated bias and rate values. The stochastic onboard clock errors were not accounted for in any way, aside from the filter's estimation of a stochastic clock rate every 9 hours. The effect of the deterministic clock calibration is shown in Figures 10 and 11. There is no obvious change to the postfit residuals, illustrating not only that the filter is able to fit the data quite well, but also that the deterministic clock bias and rate are virtually undetectable to the orbit analyst inspecting the data residuals. The orbit errors, however, show that the tangential bias has been resolved and the orbit errors are now well-represented by the (unchanged) formal solution uncertainty. In addition to demonstrate the ability to perform effective navigation with one-way GPS Doppler data, the comparison of the results with and without a deterministic clock calibration highlight the

need to assess both measurement residuals and orbit overlaps during operational navigation.

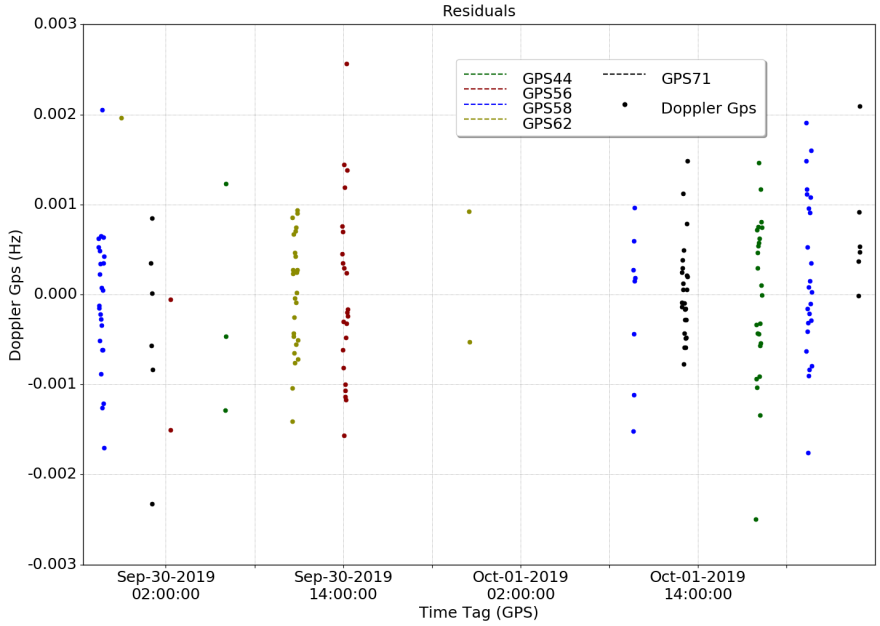

Figure 10. GPS Doppler postfit residuals (one-way Doppler with clock calibration).

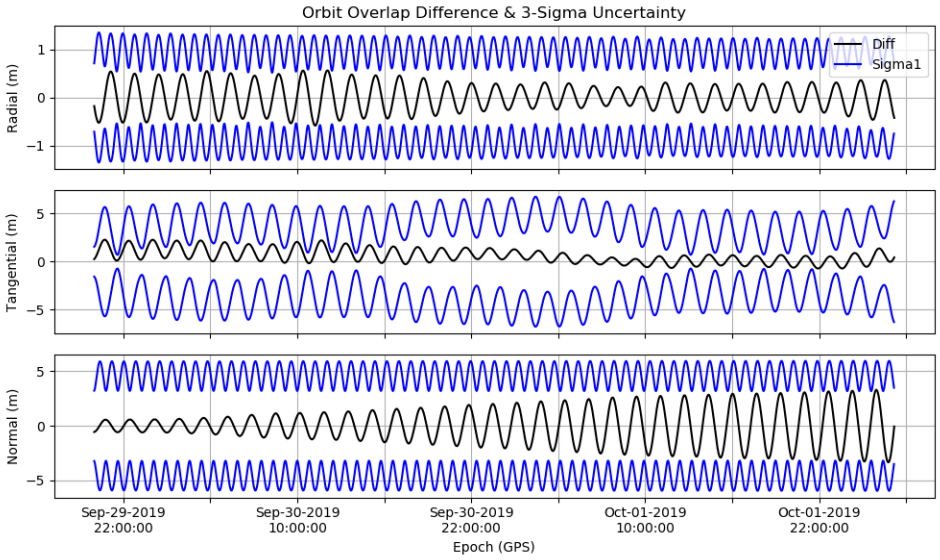

Figure 11. Orbit errors and 3-σ uncertainty envelope (one-way Doppler with clock calibration).

SUMMARY

The results of the DSAC deep space navigation analog experiment demonstrate that DSAC may be utilized as a deep space navigation instrument, provided that a calibration of the deterministic onboard clock offset and clock rate is performed. The one-way GPS Doppler and pseudo two-way

GPS Doppler solutions, both less than 10 m 3-σ formal uncertainty, are in family with current low-altitude Mars orbit reconstruction performance, and proves that one-way radiometric data can provide orbit solutions that are on par with the traditionally-utilized two-way tracking data. Furthermore, the entire navigation analog experiment was performed using the Monte navigation software currently used for deep space navigation. By carefully considering modeling effects and data processing, this experiment also demonstrated the ability to perform a proxy navigation experiment using GPS tracking data of an Earth orbiter in lieu of demonstrating the DSAC payload directly in the Mars environment. The DSAC deep space navigation analog experiment is a vital step in advancing the DSAC technology towards its ultimate role as an instrument for deep space navigation.

ACKNOWLEDGEMENTS

The authors would like to thank the entire DSAC team; each individual played a vital role in the design, build, and operation of the DSAC payload. Additional acknowledgment goes to the sponsors of the DSAC Technology Demonstration Mission, in no particular order: The National Aeronautics and Space Administration's Space Technology Mission Directorate and Space Communications and Navigation program. Finally, the authors would like to thank Tomas Martin-Mur of the Jet Propulsion Laboratory for his guidance in formulating the experiment.

The work described in this paper was carried out at the Jet Propulsion Laboratory, California Institute of Technology, under a contract with the National Aeronautics and Space Administration (80NM0018D0004).

REFERENCES

[1] N. Hinkley, J. Sherman, N. B. Phillips, M. Schioppo, N. Lemke, K. Beloy, M. Pizzocaro, C. Oats, and A. Ludlow, "An Atomic Clock with 1E-18 Instability," *Science*, Vol. 341, September 2013, pp. 1215–1218.

[2] J. D. Prestage and G. L. Weaver, "Atomic Clocks and Oscillators for Deep-Space Navigation and Radio Science," *Proceedings of the IEEE*, Vol. 95, November 2007, pp. 2235–2247.

[3] T. A. Ely, D. Murphy, J. Seubert, J. Bell, and D. Kuang, "Expected Performance of the Deep Space Atomic Clock Mission," *AAS/AIAA Space Flight Mechanics Meeting*, Santa Fe, NM, 2014.

[4] J. Ries, S. Betttadpur, R. Eanes, Z. Kang, U. Ko, C. McCullough, P. Nagel, N. Pie, S. Poole, T. Richter, H. Save, and B. Tapley, "The Combined Gravity Model GGM05C," 2016.

[5] T. D. Moyer, *Formulation for Observed and Computed Values of Deep Space Network Data Types for Navigation*. Hoboken, New Jersey: John Wiley and Sons, 2003.

[6] K. M. Larson, N. Ashby, C. Hackman, and W. Bertiger, "An Assessment of Relativistic Effects for Low Earth Orbiters: The GRACE Satellites," *Metrologia*, Vol. 44, 2007, pp. 484–490.

[7] G. Kruizinga, "M2020 Orbit Determination Assumptions," Interoffice Memorandum 392A-19-003, Jet Propulsion Laboratory, October 2017.

[8] W. Folkner, "Effect of Uncalibrated Charged Particles on Doppler Tracking," tech. rep., Jet Propulsion Laboratory, March 1994. JPL IOM 335.1-94-005.